frontiers | Frontiers in Physics

ORIGINAL RESEARCH
published: 25 August 2022
doi: 10.3389/fphy.2022.944623

High Speed RGB-Based Duobinary-Encoded Visible Light Communication System Under the Impact of Turbulences

Lin Li[1] and Abhishek Sharma[2]*

[1]*Beijing Institute of Technology, School of Optics and Photonics, Beijing, China,* [2]*Department of Electronics Technology, Guru Nana Dev University, Amritsar, India*

Recent gains in the pervasiveness of Visible Light Communication due to its ability to simultaneously provide lighting and communication solutions make it the best candidate for enabling smart city infrastructure to have seamless connectivity. The fundamental challenge of this technology is to ensure high data rate communication while meeting the lighting requirements of smart cities. This work is focused on providing high data rate capacity using visible light communication. To realize this, diffused channel modeling and channel modeling are considered. A total of six channels, each carrying 10 Gbps data are multiplexed using polarization division multiplexing and wavelength division multiplexing transmitted over a diffused channel of 1.3 m, while the ranges of 8 m under clear conditions and 5 m under heavy attenuation are reported with modeling. The reported results show the successful transmission of data in terms of bit error rate and eye diagram.

Keywords: smart city, visible light communication, polarization division multiplexing, wavelength division multiplexing, diffused channels

OPEN ACCESS

Edited by:
Muhammad Saadi,
University of Central Punjab, Pakistan

Reviewed by:
Akhilesh Kumar Pathak,
Chulalongkorn University, Thailand
Dinesh Pathak,
The University of the West Indies St. Augustine, Trinidad and Tobago

****Correspondence:***
Lin Li
linly5260@163.com

Specialty section:
This article was submitted to Optics and Photonics, a section of the journal Frontiers in Physics

Received: *15 May 2022*
Accepted: *09 June 2022*
Published: *25 August 2022*

Citation:
Li L and Sharma A (2022) High Speed RGB-Based Duobinary-Encoded Visible Light Communication System Under the Impact of Turbulences. Front. Phys. 10:944623. doi: 10.3389/fphy.2022.944623

1 INTRODUCTION

A study published in 2018 by the United Nations Department of Economic and social affairs [1] showed that more than 55% of the total world population existed in urban areas, a figure which is expected to grow by 68% in 2050. This rising urbanization makes cities complex schemes to preserve and manage. Hence, the need for systematic improvement is relevant and may provide sustainable services to the residents while ensuring their quality of life [2]. A city needs to be smart to assure these goals. The standard definition of a smart city is given as “modernization that enriches the quality of life with regard to people, governance, environment, mobility, economy, urban sustainability, and living, not essentially but primarily, based on information and communication technology” [3]. For achieving such enrichments, new means of communication are required that are greener, more cost effective, ultra-fast, and that have high data carrying capabilities.

Since the last decade, the use of optics in communication has been researched as part of greener communication. Optics in a wireless fashion (also known as optical wireless communication) garnered the attention of researchers in early 2010 and have been widely deployed for communication. Key works of optics in wireless communication are divided primarily into three sections including Inter-satellite Optical Wireless Communication [4–12] and Free space Optics (FSO) [5, 13–24]. Free Space optics have been widely deployed in providing high speed and secure communication where a wired system is a costly [25–28]. To make use of existing lighting systems for communication in smart cities, the use of visible light communication is proposed. With advantages in solid state devices, lightening sources changed from incandescent bulbs to Compact Florescent Light, and now, much advanced PN junction-based laser diode illuminators [29]. Lasers are not only greener but have energy efficiency which makes them the perfect candidate to achieve the sustainable goals of smart cities. Lasers can be switched to a very high frequency without even flickering to human eyes, and can be modulated with information signals, thereby achieving visible light communication. VLC also offers an unlicensed wide spectrum of 300 THz that offers high speed data transfers [30, 31]. The ability to integrate VLC with RF enhances their wireless transmission and smart uses in existing infrastructure, making them cost effective. VLC is primarily used in an indoor environment, provided it is a line-of-sight communication. The channel modeling is not only allowed in the use of VLC in diffused link communication but it is also being implied in navigation applications for ranging and tracking instead of GPS.

A typical VLC system consists of a transmitter and receiver while the signal is propagated in free space. As the free space channel has high attenuation, channel modeling is very crucial. Fading modeling is implemented to study the impact of attenuation such as dispersion or scattering as well as under pointing errors [32, 33]. The use of multiplexing techniques has been advised for capacity enhancement in transmission systems. Polarization division multiplexing is one technique that is used widely [34–40]. In 2019 [41], an overview of VLS system perspectives and requirements was presented. Another study, in 2020 [42], proposed the application of VLC in 6G high-speed data transmission. Another study [43] presented a survey on physical layer security for VLC systems. In another work [44], organic LED was demonstrated to carry real-time data at a speed of two Mbps experimentally. In another study [45], channel modeling was proposed to utilize VLC in vehicular tracking in an all-weather environment. In 2021 [46], researchers proposed a localization algorithm for the VLC system. In the same year [47], researchers proposed a modified grasshopper algorithm for dynamic route discovery in VLC systems. Another study [48] comprising a statistical channel model is proposed for VLC in dynamic vehicular systems. In 2022 [49], authors proposed techniques to suppress the ambient light in vehicular VLC systems. Another study [50] proposes a detection technique for jamming attacks in smart LED-based VLC systems.

In this work, a duo-binary modulation scheme was used to realize a low-cost visible light communication system. To enhance the capacity, wavelength division multiplexing along with polarization multiplexing was used over a diffused link of 1.3 m. The system was further tested with half irradiance angle and half incidence angle. The results are presented in the form of bit error rate (BER) and eye diagram. The system is also validated using a free space link. The rest of the paper is structured as follows: **Section 2** discusses System modeling for the proposed PDM-WDM-VLS system, and **Section 3** consists of Results and discussion, followed by a Conclusion in **Section 4**.

2 SYSTEM MODELING

The basic block diagram of the proposed 6×10 Gbps VLC system for smart cities is shown in **Figure 1** modeled via OptiSystem™ software. Each channel consists of 10 Gbps of data encoded in duo-binary format.

The output signal is the intensity modulated using a light source with the highest wavelengths of 630 nm (red laser), 532 nm (green laser), and 465 nm (blue laser), respectively. To enhance the capacity, the channels are multiplexed using polarization division multiplexing. The output from channels 1, 2, and 3 is given X polarization that is given 0° phase shift while the output of channels 4, 5, and 6 is given Y Polarization with a 90° phase shift. **Figure 2** indicates the polarization states, and X and Y polarizations. A pseudo random bit sequence of 10 Gbps is generated in each channel which is further encoded in duo-binary modulation format. A directly modulated laser is employed with a d.c. bias of 1 a.u. which modulates the signal from a duo-binary generator with an optical signal. The output of the first three channels is given 0° azimuthal phase shift and termed as X polarization while the other channels are given azimuthal phase shift of 90° and termed as Y (polarization as shown in **Figure 2**). The output from the X and Y polarization states is combined and transmitted over a free space channel. Two types of channel modeling are assumed in this work. First, the propagation is tested in a diffused link of 1.3 m. The transmitter is assumed to be a Lambertian disk that exposes the detector area positioned at an axial distance of h from the source.

Based on the transmitter half angle, the Lembertian order can be mathematically expressed as [51]:

$$m = \frac{-\log 2}{\log\left[cos\ \left(Transmitter\ half\ angle\right)\right]} \tag{1}$$

and concentration gain (optical) can be computed mathematically as:

$$Gain = \frac{\mathrm{I}^2}{sin\ \left(CR\right)^2} \tag{2}$$

Where the internal refractive index of the lens is given as I and field of view is given as CR.

The Gaussian optical filter is used as the receiver to collect the R, G, and B laser lights, and this filtered signal is further fed into an avalanche photo diode (APD) for detection. Photo-detector output is applied to a trans-impedance amplifier, and the amplified output is subjected to the low pass filter in order to recover the original data. The bit error rate (BER) performance is measured using a BER tester. The received signal *y(t)* is given as [52]:

$$y\ (t) = x(t) \otimes h\ (t) + n(t) \tag{3}$$

where the transmitted signal is expressed as x(t), h(t) signifies channel response, convolution is denoted as ⊗ and n(t) depicts additive white Gaussian noise (AWGN). To replicate the various attenuations, diffused channel modeling is used. The results are also compared using the same system applied in a free space environment using Gamma-Gamma channel modeling given by [53]:

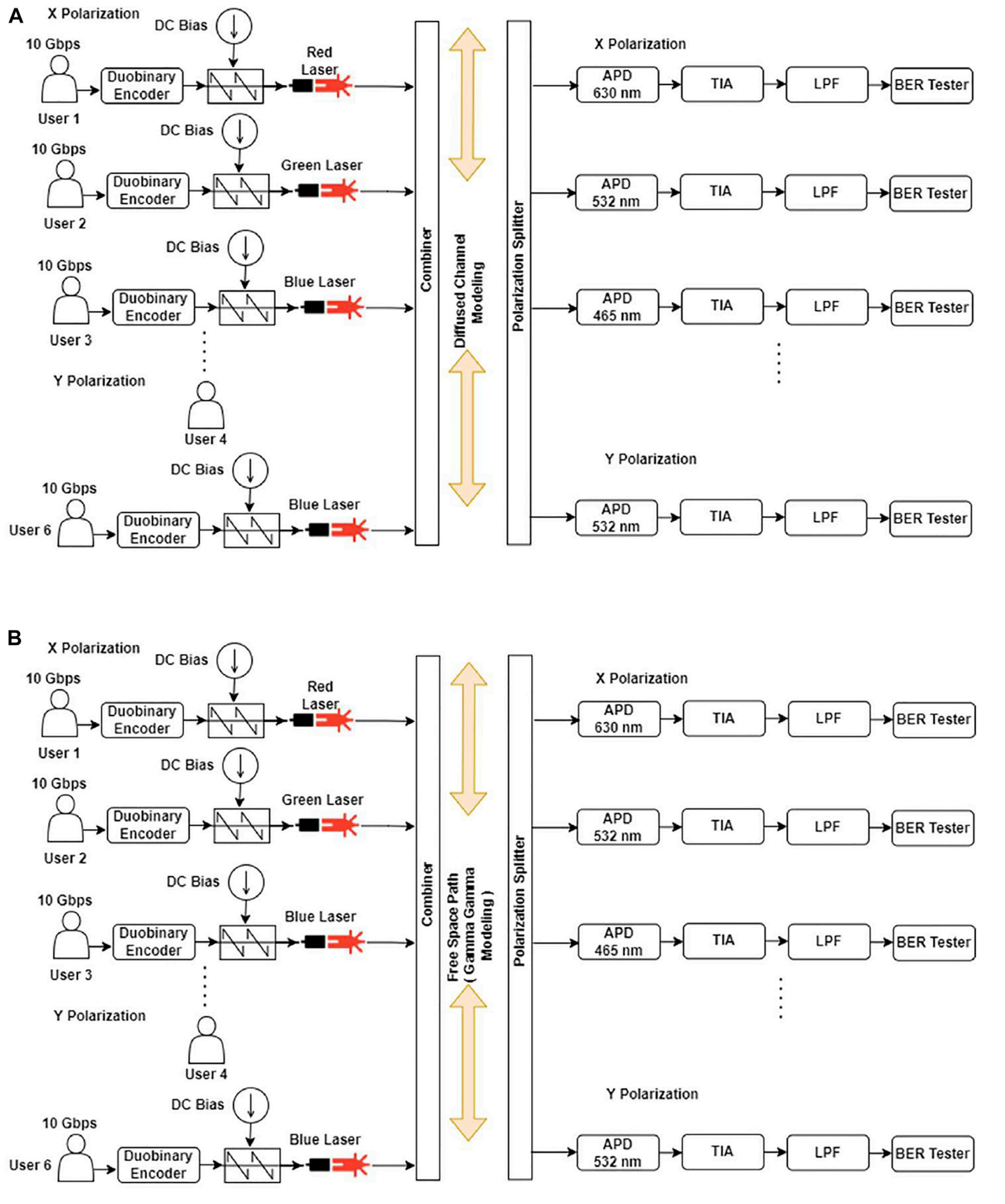

FIGURE 1 | Proposed RGB based 6 × 10 Gbps Duobinary encoded visible light communication systems **(A)** diffused modeling **(B)** Gamma-Gamma modeling.

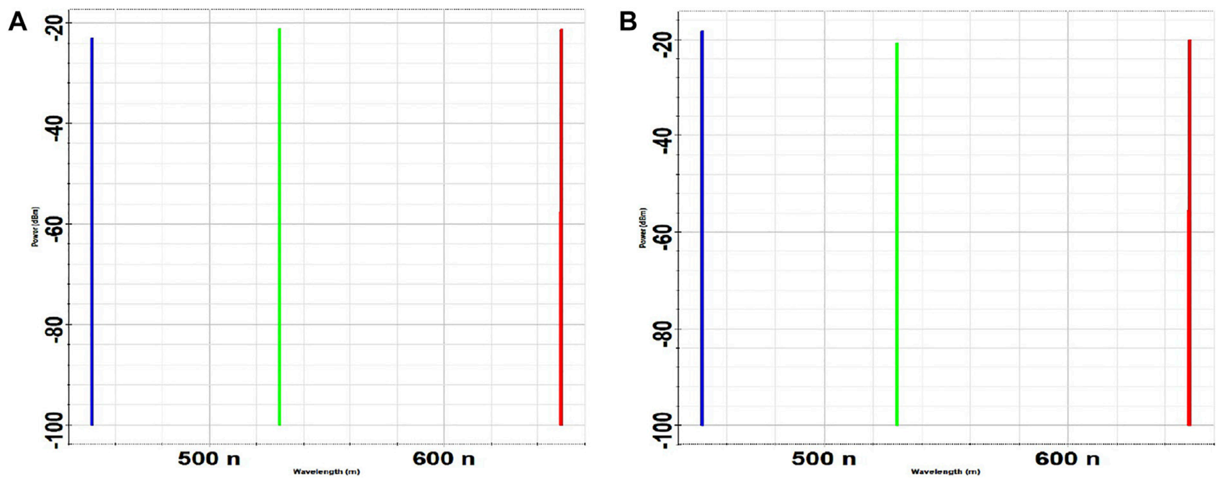

FIGURE 2 | Polarization states, **(A)** X Polarization and **(B)** Y Polarization.

TABLE 1 | System parameters.

Component	Parameter	Value
Simulation Window	Bit Rate	10 Gbps
	Time Window	3.2768e-006s
	Sample Rate	160e+009 Hz
	Sequence Length	32,768 bits
Laser	Wavelength	650 nm (Red), 530 nm (Green), and 450 nm (Blue)
	Extension Ratio	10 dB
	Power	0 dB
	Line width	10 MHz
Diffused Link	Transmitter half angle	60 deg
	Irradiance half angle	0 deg
	Incidence half angle	0 deg
	Detection surface area	1 mm^2
	Optical Concentration factor	1
	Index Concentration Factor	1.5
	Propagation delay	0 ps/m
Photo diode	Responsitivity	1.2 A/W
	Gain	3
	Thermal noise power	100e-024 W/Hz
	Dark current	10 nA
	Ionization Ratio	0.9

$$p\ (I) = \frac{2(\alpha\beta)^{\left(\frac{\alpha+\beta}{2}\right)}}{\Gamma(\alpha)\Gamma(\beta)}\, I^{\left(\alpha+\frac{\beta}{2}\right)-1} K_{\alpha-\beta}\left(2\sqrt{\alpha\beta I}\right);\quad I > 0 \tag{4}$$

where α and $ß$ represent large and small scattering eddies, K_n (.) is the second order Bessel function of the order n and Γ (.) represents the function. The parameters α and $ß$ are given by [54]:

$$\alpha = \left[exp\left(\frac{0.49\ \sigma_l^2}{\left(1 + 1.11\ \sigma_l^{\frac{12}{5}}\right)^{\frac{7}{6}}}\right) - 1\right]^{-1} \tag{5}$$

and

$$\beta = \left[exp\left(\frac{0.51\ \sigma_l^2}{\left(1 + 0.69\ \sigma_l^{\frac{12}{5}}\right)^{\frac{5}{6}}}\right) - 1\right]^{-1} \tag{6}$$

The parameters used in the numerical simulation are listed in **Table 1**.

3 RESULTS AND DISCUSSION

In this section, the results obtained from numerical simulation of the proposed PDM-WDM enabled duo-binary VLC system are presented and discussed. First, the system is tested for normal

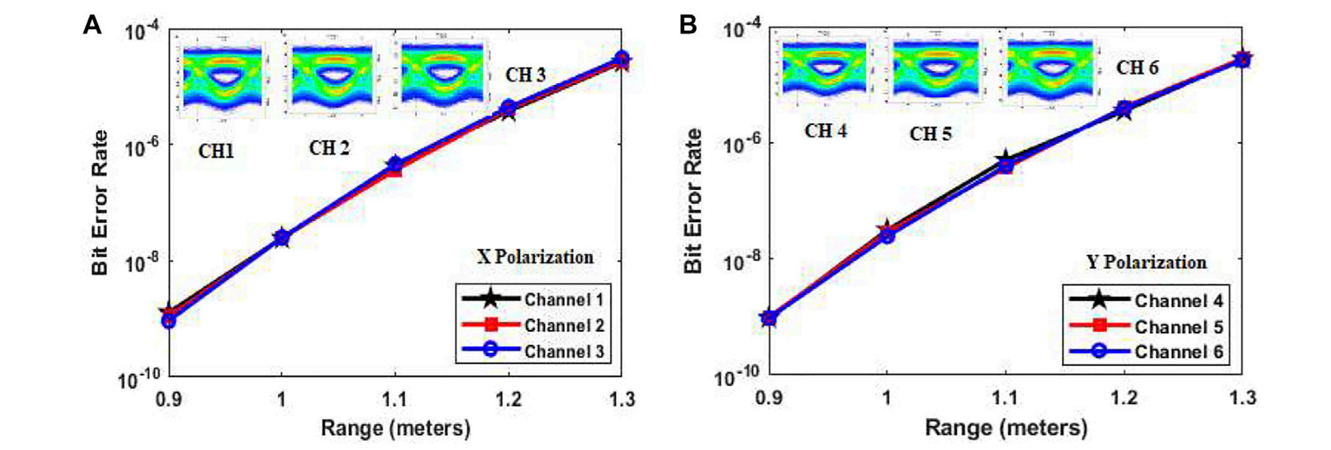

FIGURE 3 | BER vs. Transmission Range **(A)** with X polarization and **(B)** with Y Polarization.

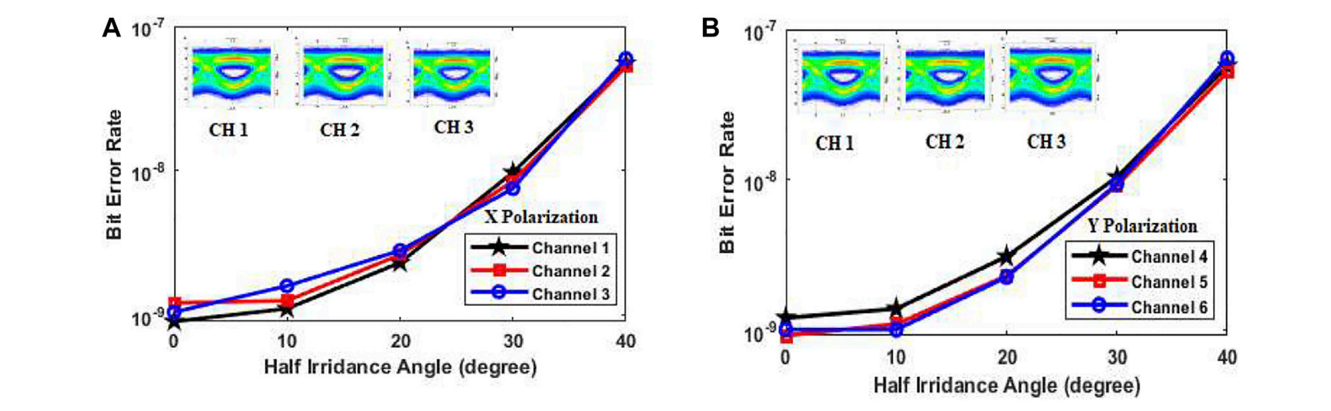

FIGURE 4 | BER vs. Half Irradiance Angle **(A)** with X polarization and **(B)** with Y Polarization.

conditions in diffused channel modeling. The system is tested for a range of 1.30 m and the results are presented in **Figure 1** in the forms of bit error rate and eye diagram.

Figure 3 depicts successful reception of VLC signal at receiver with acceptable BER which should be less than 10^{-3} for both the polarization. Channels 1, 2, and 3 have BER of 2.62×10^{-5}, $2.71 \times 10^{-5,}$ and 3.06×10^{-5} respectively with X polarization at 1.3 m. Similarly, channels 4, 5, and 6 have BER of 2.78×10^{-5}, $2.80 \times 10^{-5,}$ and 2.59×10^{-5} respectively with Y polarization at 1.3 m. Furthermore, clear eye opening depicts the successful transmission of data. The reported BER is less than 10^{-3}, which satisfies the minimum accepted BER for successful signal reception.

The system is further tested for half irradiance and half incidence angle effects on its performance. The range is kept constant at 1.30 m for all the cases. **Figure 4** depicts the successful reception of the signal in which the BER of 10^{-8} for a half irradiance angle of up to 40° is reported. Channels 1, 2, and 3 have BER of 5.53×10^{-8}, $5.24 \times 10^{-8,}$ and 5.97×10^{-8} respectively with X polarization at 40°. Similarly, channels 4, 5, and 6 have a BER of 5.72×10^{-8}, $5.21 \times 10^{-8,}$ and 6.42×10^{-8} respectively with Y polarization at 40°. Again the numerically calculated BER is less than 10^{-3}, which satisfies the minimum acceptable BER condition for successful transmission along with clear eye opening in eye diagrams.

Figure 5 depicts the successful reception of the signal in which a BER of 10^{-5} with respect to half incidence angle up to 60° is reported. Channels 1, 2, and 3 have BER of 1.60×10^{-5}, $1.59 \times 10^{-5,}$ and 1.74×10^{-5} respectively with X polarization at 60°. Similarly, channels 4, 5, and six have a BER of 1.81×10^{-5}, 1.71×10^{-5}, and 1.63×10^{-5} respectively with Y polarization at 60°. The reported BER is less than 10^{-3}, which satisfies the minimum accepted BER for successful signal reception supported by clear eye openings.

The proposed system is also tested in gamma-gamma modeling for a free space environment. **Figure 6** presents the BER vs. range plot under clear conditions up to the range of 8 m.

Figure 6 depicts the successful reception of the signal in which a BER of 10^{-5} with a respected range of 8 m is reported. Channels 1, 2, and 3 have a BER of 1.30×10^{-5}, $1.59 \times 10^{-5,}$ and 1.43×10^{-5} respectively with X polarization at 8 m. Similarly, channels 4, 5, and six have BER of 1.91×10^{-5}, $1.35 \times 10^{-5,}$ and 1.32×10^{-5} respectively with Y polarization at 8 m. As the system interacts

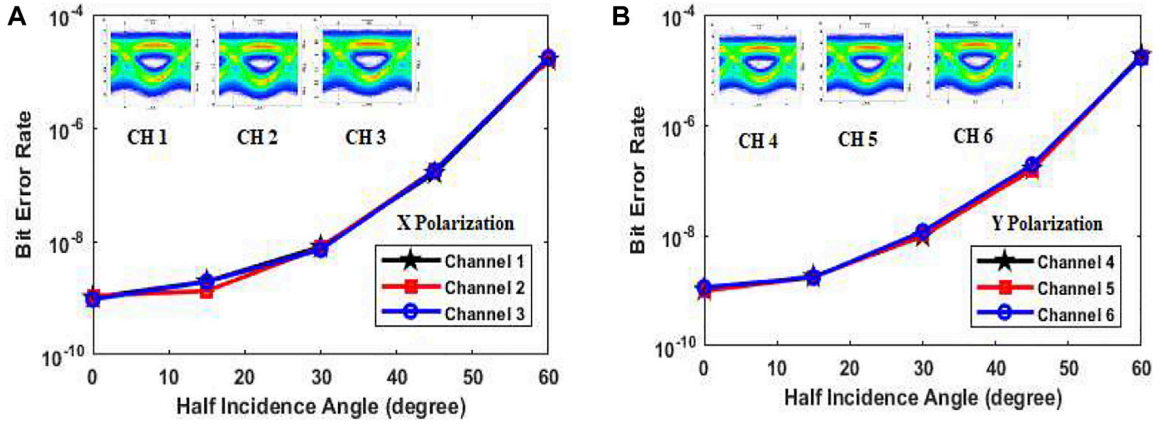

FIGURE 5 | BER vs. Half Incidence Angle **(A)** with X polarization and **(B)** with Y Polarization.

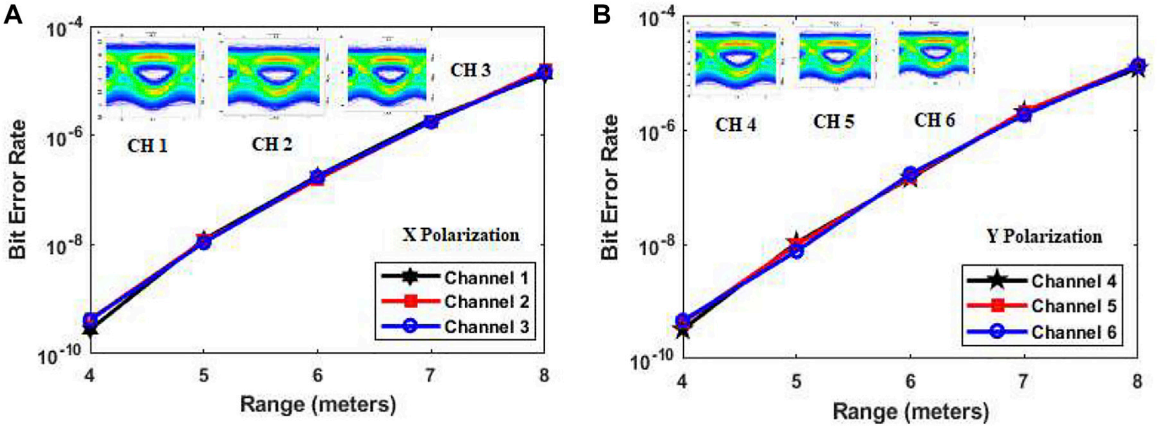

FIGURE 6 | BER vs. Range up to 8 m under clear conditions **(A)** with X polarization and **(B)** with Y Polarization.

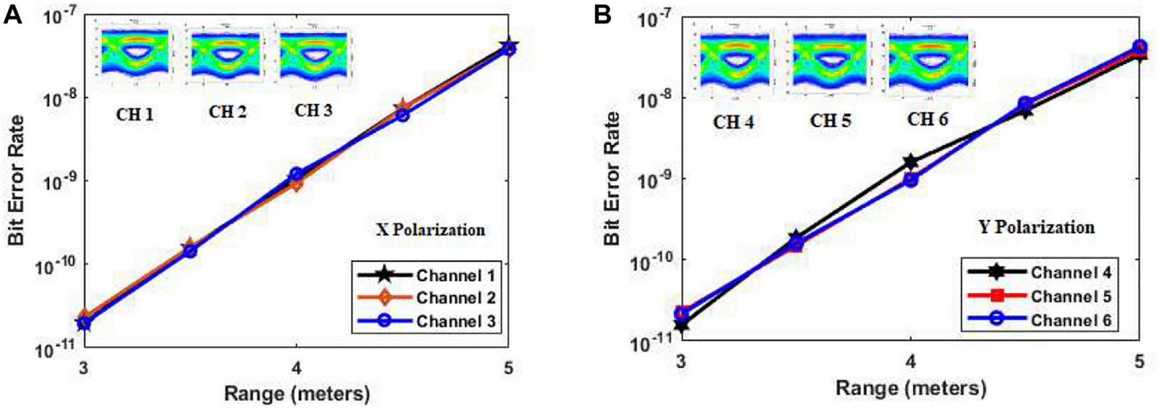

FIGURE 7 | BER vs. Range up to 5 m with heavy attenuation **(A)** with X polarization and **(B)** with Y Polarization.

with various atmospheric conditions in a free space environment, heavy attenuation of 75 dB is introduced. **Figure 7** shows the successful reception of the signal in which a BER of 10^{-8} with a respected range of 5 m is reported. Channels 1, 2, and 3 have a BER of 4.20×10^{-8}, $3.76 \times 10^{-8,}$ and 3.77×10^{-8} respectively with X polarization at 5 m. Similarly, channels 4, 5, and six have BER of 3.37×10^{-8}, $3.82 \times 10^{-8,}$ and 4.22×10^{-8} respectively with Y polarization at 5 m. From the mentioned values, it is clear that obtained BER is less than 10^{-3} satisfies the minimum accepted BER for successful signal reception.

Clear eye opening in both the cases further explains the successful reception of data at the receiver side.

4 CONCLUSION

In this work, PDM-WDM enabled VLC system under the impact of different channel modeling for a smart city is proposed. VLC is implemented using RGB Lasers with wavelengths of 650 nm (Red), 530 nm (Green), and 450 nm (Blue) respectively to transmit 10 Gbps data in six channels. The reported results show the successful transmission of data in the diffused link of 1.3 m. Furthermore, the proposed system is tested under the impact of half irradiance up to 40° and half incidence angle up to 60°. The successful transmission is reported in terms of BER, which is below the FEC limit of $3.8 \times 10^{-3,}$ and the Eye diagram. The proposed system is tested in the Gamma-Gamma channel with ranges of 8 m in clear atmospheric conditions and 5 m under heavy attenuation. In future work, real time test beds will be considered, to replicate the simulative modeled system in experimental studies.

DATA AVAILABILITY STATEMENT

The original contributions presented in the study are included in the article/supplementary material, further inquiries can be directed to the corresponding author.

AUTHOR CONTRIBUTIONS

All authors listed have made a substantial, direct, and intellectual contribution to the work and approved it for publication.

FUNDING

This work was supported by the "Ten Thousand Million" Engineering Technology Major Special Support Action Plano of Heilongjiang Province, China (SC2021ZX02A0040), and the National Key Research and Development Program of China under Grant No. 2018YFB1305700 and Quanzhou Scientific and Technological Planning Projects under Grant No. 2019CT009.

REFERENCES

1. United Nations. *World urbanization prospects: The 2018 revision, highlights*. New York: Economic Analysis and Policy Division, Department of Economic and Social Affairs, United Nations Secretariat (2018).
2. Cerruela García G, Luque Ruiz I, Gómez-Nieto MÁ. State of the art, trends and future of bluetooth low energy, near field communication and visible light communication in the development of smart cities. *Sensors* (2016) 16:1968. doi:10.3390/s16111968
3. Anthopoulos LG, Reddick CG. Understanding electronic government research and smart city: A framework and empirical evidence. *Inf Polity* (2016) 21: 99–117. doi:10.3233/ip-150371
4. Sharma A, Malhotra J, Chaudhary S, Thappa V. Analysis of 2 × 10 Gbps MDM enabled inter satellite optical wireless communication under the impact of pointing errors. *Optik* (2021) 227:165250. doi:10.1016/j.ijleo.2020.165250
5. Sharma A, Parmar A, Sood P, Dhasratan V, Guleria C. Performance analysis of free space optics and inter-satellite communicating system using multiplexing techniques – a review. *J Opt Commun* (2019) 42:465–70. doi:10.1515/joc-2018-0107
6. Chaudhary S, Tang X, Sharma A, Lin B, Wei X, Parmar A. A cost-effective 100 Gbps SAC-OCDMA–PDM based inter-satellite communication link. *Opt Quan Electron* (2019) 51:148. doi:10.1007/s11082-019-1864-2
7. Chaudhary S, Sharma A, Singh V. Optimization of high speed and long haul inter-satellite communication link by incorporating differential phase shift key and orthogonal frequency division multiplexing scheme. *Optik* (2019) 176: 185–90. doi:10.1016/j.ijleo.2018.09.037
8. Chaudhary S, Kapoor R, Sharma A. Empirical evaluation of 4 QAM and 4 PSK in OFDM-based inter-satellite communication system. *J Opt Commun* (2019) 40:143–7. doi:10.1515/joc-2017-0059
9. Chaudhary S, Sharma A, Chaudhary N. 6 × 20 Gbps hybrid WDM–PI inter-satellite system under the influence of transmitting pointing errors. *J Opt Commun* (2016) 37:375–9. doi:10.1515/joc-2015-0099
10. Chaudhary S, Sharma A, Neetu N. 6 x 20Gbps long reach WDM-PI based high altitude platform inter-satellite communication system. *Int J Comput Appl* (2015) 122:41–5. doi:10.5120/21861-5192
11. Sharma A, Kumar V, Gupta V. A review on inter-satellite optical wireless communication. *Int J Comput Appl* (2018) 180:13–7. doi:10.5120/ijca2018916238
12. Sharma A, Kumar V, C. C. High speed and long reach DPSK-OFDM-is-OWC under impact of space turbulences. *Int J Comput Appl* (2018) 975:27–30. doi:10.5120/ijca2018916227
13. Chaudhary S, Sharma A, Tang X, Wei X, Sood P. A cost effective 100 Gbps FSO system under the impact of fog by incorporating OCDMA-PDM scheme. *Wirel Pers Commun* (2021) 116:2159–68. doi:10.1007/s11277-020-07784-3
14. Sharma A, Chaudhary S, Thakur D, Dhasratan V. A cost-effective high-speed radio over fibre system for millimeter wave applications. *J Opt Commun* (2020) 41:177–80. doi:10.1515/joc-2017-0166
15. Shakthi Murugan KH, Sharma A, Malhotra J. Performance analysis of 80 Gbps Ro-FSO system by incorporating hybrid WDM-MDM scheme. *Opt Quan Electron* (2020) 52:505. doi:10.1007/s11082-020-02613-0
16. Chaudhary S, Chauhan P, Sharma A. High speed 4× 2.5 Gbps-5 GHz AMI-WDM-RoF transmission system for WLANs. *J Opt Commun* (2019) 40:285–8. doi:10.1515/joc-2017-0082
17. Zhou Z, Zhang H, Lin C, Sharma A. Performance analysis of duobinary and CSRZ modulation based polarization interleaving for high-speed WDM-FSO transmission system. *J Opt Commun* (2018) 1:147–52. doi:10.1515/joc-2018-0188
18. Sood P, Sharma A, Chandni Ms. Analysis of FSO system and its challenges - a review. *Int J Comput Appl* (2018) 179:42–5. doi:10.5120/ijca2018917353
19. Sharma A, Thakur D. A review on WLANs with radio-over-fiber technology. *Int J Electron Commun Eng (Ijece)* (2017) 6:1–6.
20. Sharma A, Rana S. Implementation of radio over fiber technology with different filtration techniques. *Int J Res Appl Sci Eng Tech* (2017) V:783–9. doi:10.22214/ijraset.2017.8110

21. Sharma A, Chauhan P. A study of radio over fiber technology in WLAN applications. *Int J Res Appl Sci Eng Tech* (2017) V:416–20. doi:10.22214/ijraset.2017.8058
22. Chaudhary S, Thakur D, Sharma A. 10 Gbps-60 GHz RoF transmission system for 5 G applications. *J Opt Commun* (2019) 40:281–4. doi:10.1515/joc-2017-0079
23. Sharma A, Chaudhary S, Malhotra J, Parnianifard A, Kumar S, Wuttisittikulkij L. Impact of bandwidth on range resolution of multiple targets using photonic radar. *IEEE Access* (2022) 10:47618–27. doi:10.1109/access.2022.3171255
24. Sharma A, Chaudhary S, Malhotra J, Parnianifard A, Wuttisittikulkij L. Measurement of Target range and Doppler shift by incorporating PDM-enabled FMCW-based photonic radar. *Optik* (2022) 262:169191. doi:10.1016/j.ijleo.2022.169191
25. Padhy JB, Patnaik B. Link performance evaluation of terrestrial FSO model for predictive deployment in Bhubaneswar smart city under various weather conditions of tropical climate. *Opt Quan Electron* (2021) 53:82. doi:10.1007/s11082-020-02702-0
26. Singh H, Mittal N, Miglani R, Singh H, Gaba GS, Hedabou M. Design and analysis of high-speed free space optical (FSO) communication system for supporting fifth generation (5G) data services in diverse geographical locations of India. *IEEE Photon J* (2021) 13:1–12. doi:10.1109/jphot.2021.3113650
27. Kumar DA, Sangeetha RG. Performance analysis of power series based gamma–gamma fading M-ary PSK MIMO/FSO link with atmospheric turbulence and pointing errors. *Telecommun Syst* (2022) 79:481–502. doi:10.1007/s11235-021-00835-5
28. Saber MJ, Rajabi S. On secrecy performance of millimeter-wave RF-assisted FSO communication systems. *IEEE Syst J* (2021) 15:3781–8. doi:10.1109/jsyst.2021.3065885
29. Pan Z, Lang T, Li C, Di M, Chen G, Kalay Y, et al. Visible light communication cyber-physical systems-on-chip for smart cities. *J Commun* (2019) 14 (12): 1141–6. doi:10.12720/jcm.14.12.1141-1146
30. Zhou Z, Lin B, Tang X, Chaudhary S, Lin C, Zhang H. Performance comparison of DFT-OFDM, DCT-OFDM, and DWT-OFDM for visible light communications. In: Procedding of the 17th International Conference on Optical Communications and Networks (ICOCN2018); Feb 2019; Zhuhai, China (2019). p. 397–402.
31. Zhou Z, Lin B, Tang X, Chaudhary S, Lin C, Zhang H, et al. Experimental demonstration of PAM-DWMT for visible light communications. In: Procedding of the Asia Communications and Photonics Conference; October 2018; Hangzhou, China. IEEE (2018). Su4D. 5.
32. Chaudhary S, Amphawan A, Nisar K. Realization of free space optics with OFDM under atmospheric turbulence. *Optik* (2014) 125:5196–8. doi:10.1016/j.ijleo.2014.05.036
33. Chaudhary S, Amphawan A. The role and challenges of free-space optical systems. *J Opt Commun* (2014) 35:327–34. doi:10.1515/joc-2014-0004
34. Aravindan N, Raja AS, Selvendran S, Balasubramonian M. Dual channel indoor VLC system using PDM scheme: An investigation. *Opt Quan Electron* (2022) 54:229. doi:10.1007/s11082-022-03634-7
35. Yang Y-C, Yeh C-H, Liaw S-K, Chow C-W, Hsu W-H, Wang B-Y. Analysis and investigation of dual-polarized color LED based visible light communication system. *Photonics* (2021) 8:210. doi:10.3390/photonics8060210
36. Mathur H, Deepa T. A novel precoded digitized OFDM based NOMA system for future wireless communication. *Optik* (2022) 259:168948. doi:10.1016/j.ijleo.2022.168948
37. Wang Z, Wei Z, Cai Y, Wang L, Li M, Liu P, et al. Encapsulation-enabled perovskite–PMMA films combining a micro-LED for high-speed white-light communication. *ACS Appl Mater Inter* (2021) 13:54143–51. doi:10.1021/acsami.1c15873
38. Fang X, Zhu M, Suo Z, Fu Y, Ding D, Chen Y, et al. Nonlinear suppression for polarization division multiplexed optical OFDM/OQAM systems. *Opt Fiber Tech* (2022) 69:102818. doi:10.1016/j.yofte.2022.102818
39. Sharma A, Malhotra J. Simulative investigation of FMCW based optical photonic radar and its different configurations. *Opt Quan Electron* (2022) 54:233. doi:10.1007/s11082-022-03578-y
40. Sharma A, Chaudhary S, Malhotra J, Saadi M, Otaibi SA, Nebhen J, et al. A cost-effective photonic radar under adverse weather conditions for autonomous vehicles by incorporating frequency modulated direct detection scheme. *Front Phys* (2021) 9:467. doi:10.3389/fphy.2021.747598
41. Rehman SU, Ullah S, Chong PHJ, Yongchareon S, Komosny D. Visible light communication: A system perspective—overview and challenges. *Sensors* (2019) 19:1153. doi:10.3390/s19051153
42. Chi N, Zhou Y, Wei Y, Hu F. Visible light communication in 6G: Advances, challenges, and prospects. *IEEE Veh Technol Mag* (2020) 15:93–102. doi:10.1109/mvt.2020.3017153
43. Arfaoui MA, Soltani MD, Tavakkolnia I, Ghrayeb A, Safari M, Assi CM, et al. Physical layer security for visible light communication systems: A survey. *IEEE Commun Surv Tutorials* (2020) 22:1887–908. doi:10.1109/comst.2020.2988615
44. Minotto A, Haigh PA, Łukasiewicz ŁG, Lunedei E, Gryko DT, Darwazeh I, et al. Visible light communication with efficient far-red/near-infrared polymer light-emitting diodes. *Light Sci Appl* (2020) 9:70. doi:10.1038/s41377-020-0314-z
45. Karbalaygh areh M, Miramirkhani F, Eldeeb HB, Kizilirmak RC, Sait SM, Uysal M. Channel modelling and performance limits of vehicular visible light communication systems. *IEEE Trans Veh Technol* (2020) 69:6891–901. doi:10.1109/tvt.2020.2993294
46. Dawood MA, Saleh SS, El-Badawy E-SA, Aly MH. A comparative analysis of localization algorithms for visible light communication. *Opt Quan Electron* (2021) 53:108. doi:10.1007/s11082-021-02751-z
47. Vadivel S, Konda S, Balmuri KR, Stateczny A, Parameshachari BD. Dynamic route discovery using modified grasshopper optimization algorithm in wireless ad-hoc visible light communication network. *Electronics* (2021) 10:1176. doi:10.3390/electronics10101176
48. Alsalami FM, Ahmad Z, Zvanovec S, Haigh PA, Haas OCL, Rajbhandari S. Statistical channel modelling of dynamic vehicular visible light communication system. *Vehicular Commun* (2021) 29:100339. doi:10.1016/j.vehcom.2021.100339
49. Ahmed M, Atta MA, Farmer J, Dawy Z, Brien DO, Bermak A. Multidomain suppression of ambient light in visible light communication transceivers. *IEEE Trans Intell Transp Syst* (2022) 1–10. doi:10.1109/tits.2022.3162635
50. Park SH, Joo S, Lee IG. Secure visible light communication system via cooperative attack detecting techniques. *IEEE Access* (2022) 10:20473–85. doi:10.1109/access.2022.3151627
51. Barry JR *Wireless infrared communications*, 280. Springer Science & Business Media (1994).
52. Qiu Y, Chen HH, Meng WX. channel modeling for visible light communications—A survey. *Wirel Commun Mob Comput* (2016) 16: 2016–34. doi:10.1002/wcm.2665
53. Andrews LC, Phillips RL *Laser beam propagation through random media*, 152. WA: SPIE press Bellingham (2005).
54. Ghassemlooy Z, Popoola W, Rajbhandari S. *Optical wireless communications: System and channel modelling with Matlab®*. London: CRC Press (2019).

Conflict of Interest: The authors declare that the research was conducted in the absence of any commercial or financial relationships that could be construed as a potential conflict of interest.

Publisher's Note: All claims expressed in this article are solely those of the authors and do not necessarily represent those of their affiliated organizations, or those of the publisher, the editors and the reviewers. Any product that may be evaluated in this article, or claim that may be made by its manufacturer, is not guaranteed or endorsed by the publisher.